available at www.sciencedirect.com

ScienceDirect

journal homepage: www.ejconline.com

MicroRNA-130b regulates the tumour suppressor RUNX3 in gastric cancer

Kin Wai Lai [a], King Xin Koh [a], Marie Loh [a], Kotaro Tada [a], Manish Mani Subramaniam [a], Xn Yii Lim [a], Aparna Vaithilingam [a], Manuel Salto-Tellez [a,b], Barry Iacopetta [c], Yoshiaki Ito [a], Richie Soong [a,b,], the Singapore Gastric Cancer Consortium*

[a] *Cancer Science Institute of Singapore, Centre for Life Sciences #02-15, 28 Medical Drive, National University of Singapore, Singapore 117456, Singapore*

[b] *Department of Pathology, Yong Loo Lin School of Medicine, National University of Singapore, 5 Lower Kent Ridge Rd., Singapore 119074, Singapore*

[c] *School of Surgery, The University of Western Australia, 35 Stirling Highway, Crawley 6009, Australia*

ARTICLE INFO

Article history:
Received 10 November 2009
Received in revised form 20 January 2010
Accepted 26 January 2010
Available online 20 February 2010

Keywords:
RUNX3
MicroRNA
miR-130b
Gastric cancer
Tumour suppressor
Epigenetics

ABSTRACT

Aim: Accumulating evidence indicates that RUNX3 is an important tumour suppressor that is inactivated in many cancer types. This study aimed to assess the role of microRNA (miRNA) in the regulation of *RUNX3*.

Methods: Four bioinformatic algorithms were used to predict miRNA binding to *RUNX3*. The correlation between candidate miRNAs and *RUNX3* expression in cell lines was determined by real-time reverse transcriptase quantitative PCR (RT-qPCR) and Western blot. Candidate miRNAs were tested for functional effects through transfection of miRNA precursors and inhibitors, and monitoring cell viability, apoptosis and *Bim* expression. miRNA and *RUNX3* expression, *RUNX3* methylation and RUNX3 protein levels were assessed in gastric tissue by RT-qPCR, Methylight analysis and immunohistochemistry, respectively.

Results: Bioinformatics, gene and protein expression analysis in eight gastric cell lines identified miR-130b as the top candidate miRNA for RUNX3 binding. Overexpression of miR-130b increased cell viability, reduced cell death and decreased expression of *Bim* in TGF-β mediated apoptosis, subsequent to the downregulation of RUNX3 protein expression. In 15 gastric tumours, miR-130b expression was significantly higher compared to matched normal tissue, and was inversely associated with RUNX3 hypermethylation.

Conclusion: Attenuation of RUNX3 protein levels by miRNA may reduce the growth suppressive potential of RUNX3 and contribute to tumourigenesis.

1. Introduction

RUNX3 has been identified as a critical tumour suppressor in many human cancer types through the work of our laboratory and others.[1–3] RUNX3 knockout mice developed gastric hyperplasia, an early precursor of gastric cancer.[2] Gastric epithelial cells derived from RUNX3$^{-/-}$p53$^{-/-}$ mice induced the formation of tumours when inoculated into nude mice, while those derived from RUNX3$^{+/+}$p53$^{-/-}$ mice did not. Tumourigenicity of human gastric cancer cell lines in nude mice was

* *Corresponding author:* Address: Cancer Science Institute of Singapore, Centre for Life Sciences #02-15, 28 Medical Drive, National University of Singapore, Singapore 117456, Singapore. Tel.: +65 65168055; fax: +65 68739664.
E-mail address: csirs@nus.edu.sg (R. Soong).

0959-8049/$ - see front matter
doi:10.1016/j.ejca.2010.01.036

inversely related to their level of RUNX3 expression, and a mutation (R122C) occurring within the conserved Runt domain eliminates the tumour suppressive activity of RUNX3. RUNX3 is also a potent activator of many developmental and homeostatic signalling components linked to tumour suppression such as cyclin-dependent kinase inhibitor CDKN1A ($p21^{WAF1/Cip1}$)[4] and pro-apoptotic *Bim*.[5] Recent results indicate that RUNX3 forms a ternary complex with β-catenin/TCF4 and attenuates the Wnt signalling pathway.[1]

Other studies have shown that RUNX3 expression is significantly reduced in many human tumour types including gastric cancers and gastric pre-neoplastic lesions[2] as well as colorectal,[6] breast,[7] endometrial,[8] oral squamous cell[9] and oesophageal squamous cell carcinomas.[10] Moreover, inactivation of RUNX3 has been correlated with advanced disease stage and poor prognosis.[6,11]

The downregulation of RUNX3 has been attributed to a number of mechanisms, including hypermethylation of its promoter region,[2] cytoplasmic mislocalisation,[12] histone modification[13] and hemizygous deletion.[14] However, there remains a proportion of tumours that show reduced RUNX3 expression in the absence of these mechanisms, suggesting that other factors may be involved in the regulation of RUNX3.

MicroRNAs (miRNAs) are recently characterised, highly conserved, small RNA molecules of approximately 21–25 nucleotides encoded in the genomes of plants and animals.[15] They suppress gene expression either by repressing translation or by direct sequence-specific cleavage through the action of the RNA-induced silencing complex (RISC) following binding to the 3′-untranslated region (3′UTR) of mRNA.[16] Differential expression of miRNA between tumour tissue and normal tissue has been observed in various cancer types[17] suggesting a possible link between miRNA expression and the development of cancer. miRNAs have been observed to regulate both oncogenes, such as ras,[18] and tumour suppressor genes, such as PTEN.[19]

In exploratory analysis using bioinformatic algorithms, the RUNX3 3′UTR was found to contain numerous potential miRNA-binding sites, indicating that miRNA may play a role in regulating RUNX3 expression. The aims of this study were to determine whether RUNX3 is a target of miRNA regulation and to evaluate the role of this mechanism in gastric cancer.

2. Materials and methods

2.1. Selection of candidate miRNAs

Candidate miRNAs for binding to RUNX3 were identified using four web-based bioinformatic algorithms. TargetScan, PicTar and miRanda predict miRNA-binding sites based on complementarity of nucleotide sequence to the 3′-untranslated region of RUNX3 mRNA. miRBase Target is based on miRanda algorithms.[20]

2.2. Cell lines

Eight gastric cancer cell lines were obtained from American-Type Culture Collection (Manassas, VA) (AGS, SNU1, SNU5 and SNU16) and Japanese Collection of Research Bioresources (Osaka, Japan) (AZ521, MKN7, MKN28, MKN45) and were maintained in Dulbecco's Modified Eagle's Medium containing 10% foetal bovine serum and 1× Penicillin/Streptomycin. Total RNA, including miRNA, was extracted using the *mir*Vana™ miRNA isolation kit (Ambion, Austin, TX) while protein was extracted with RIPA lysis buffer (Santa Cruz Biotechnology, Santa Cruz, CA) after harvesting of the cells.

2.3. Clinical samples

Formalin-fixed, paraffin-embedded tissue blocks of tumour and matched normal tissue from 15 cases of gastric cancer were obtained from the Department of Pathology of the National University Hospital System according to an institutionally approved protocol. Genomic DNA was extracted from 4 μm sections according to the methods described previously.[21] Total RNA, including miRNA, was extracted from 20 μm sections using the RecoverAll™ total nucleic acid isolation kit (Ambion).

2.4. Real-time reverse transcriptase quantitative PCR (RT-qPCR)

For the gene expression of RUNX3 (Hs00231709_m1), *BimL* + *BimEL* (Hs00197982_m1) and all *Bim*-splicing variants (Hs00708019_s1), 500 ng of total RNA was reverse transcribed using the high-capacity cDNA reverse transcription kit (Applied Biosystems, Foster City, CA), and analysed by RT-qPCR on the ABI7900 Fast real-time PCR system (ABI) using the TaqMan® gene expression assay (ABI) normalised with β-actin (Hs99999903_m1). For the gene expression of candidate miRNAs, 100 ng of total RNA was reverse transcribed by their respective stem-loop RT primers, followed by RT-qPCR on the ABI7900HT Fast real-time PCR system using the TaqMan® microRNA assay (ABI) and normalised with RNU48. miR-130b was considered to be overexpressed when the relative ratio was greater than 2.0. All PCR reactions were performed in duplicate.

2.5. Western blot

The cells were harvested, washed once with 1× PBS and lysed in 100 μl of RIPA lysis buffer. Twenty micrograms of the protein extract were separated on a 12% polyacrylamide gel and transferred to PVDF membrane. The primary antibody for the detection of human RUNX3 was a mouse IgG antibody validated in the previous experiments.[12] Primary antibodies for Bim (sc-11425) and β-actin (sc-47778) and the corresponding HRP-conjugated secondary antibodies (sc-2004, sc-2005) were purchased from Santa Cruz Biotechnology (Santa Cruz, CA).

2.6. Overexpression and inhibition of miR-130b

The cells were transfected with 25 nM of the miR-130b precursor molecules or 50 nM of the miR-130b inhibitor molecules (ABI) by the reverse transfection method using the siPORT™ *NeoFX*™ transfecting reagent (ABI). Non-transfected cells and cells transfected with a non-expressing miRNA precursor were also examined in parallel as controls.

2.7. Trypan blue cell count

The cells were seeded at 5×10^4 cells/well in a 24-well microtiter plate transfected with miRNA precursors or inhibitors and incubated for 72 h. Subsequently, 1 ng/ml recombinant human TGF-β was added and incubated for 16, 24, 32, 40 and 48 h, before resuspension of cells at a concentration of 1×10^5 cells/ml. Equal volumes of trypan blue and cell suspension were mixed and counted in a Neubauer chamber. The results were expressed as the percentage of viable cells amongst the total cells counted.

2.8. Cell viability assay

The cell viability was assessed using the Promega CellTiter 96® AQueous non-radioactive cell proliferation assay (Madison, WI). Briefly, the cells were seeded at 2000 cells/well in a 96-well microtiter plate and transfected with the miRNA precursors or inhibitors. Recombinant human TGF-β (R&D Systems, Minneapolis, MN) at 1 ng/ml was added 24 h after subculture and the cells were further incubated for 48 and 72 h. After incubation, 20 μl of the combined MTS/PMS solution was added to 100 μl of cells and the cells were then incubated for 2 h at 37 °C in a humidified, 5% CO_2 atmosphere. The absorbance of the wells was read at 490 nm using the Benchmark microplate reader (Bio-Rad, Hercules, CA).

2.9. Detection of apoptosis and cell death

Apoptosis and cell death were assessed using the Annexin V-FITC apoptosis detection kit (BD Pharmingen, San Jose, CA). Briefly, the cells were seeded at 1.25×10^5 cells/ml in a 6-well plate transfected with the miRNA precursors or inhibitors and incubated for 72 h. TGF-β (R&D Systems, Minneapolis, MN) at 1 ng/ml was then added and the cells were incubated for further 16 h before harvesting. The cells were then washed twice with 1× PBS and resuspended in 1× Annexin V-binding buffer at a concentration of 1×10^6 cells/ml. One hundred microlitres of the cell suspension was incubated with 5 μl of Annexin V-FITC and 5 μl of propidium iodide in the dark for 15 min at room temperature. The samples were then analysed on the FACSCalibur™ flow cytometer (BD Biosciences, San Jose, CA) after the addition of 400 μl of 1× binding buffer at the end of incubation. The results were expressed as the percentage of apoptotic cells and non-viable cells amongst the total cells counted.

2.10. Immunohistochemistry

Immunhistochemistry was performed according to the methods described previously.[12] Briefly, 4 μm tissue sections underwent antigen retrieval in target retrieval solution (Dako, Glostrup, Denmark) by pressure cooking at 121 °C for 5 min in a microwave histoprocessor (Milestone, Sorisole, Italy). This was followed by peroxidase blocking in 3% H_2O_2 for 5 min and protein blocking with normal goat serum for 10 min. The sections were then incubated overnight with the RUNX3 monoclonal antibody R1E10 diluted 1:3000 in the Dako antibody diluent (Dako). The sections were then incubated with biotinylated secondary antibody and peroxidase-conjugated strepavidin using the Dako Real detection system and diaminobenzidine (Dako) according to the manufacturer's instructions. Negative controls in which the primary antibody was substituted with antibody diluent were also analysed. Staining intensity in both the nucleus and cytoplasm was assessed by experienced pathologists and graded as absent (0), weak (1+), moderate (2+) or strong (3+).

2.11. DNA Methylation analysis

One microgram of genomic DNA was treated with sodium bisulphite using the EZ DNA methylation™ kit (Zymo Research, Orange, CA), and subsequently analysed for RUNX3 methylation by the MethyLight technique as described previously.[22] The level of methylation was calculated as a percentage of methylated reference (PMR) using SssI-treated human genomic DNA as the reference. Hypermethylation was defined as PMR > 4.

2.12. Statistical analysis

All statistical analyses were carried out in SPSS version 16.0 (Chicago, IL), with the exception of calculations for polyserial and polychoric correlation coefficients, which were performed using R version 2.7.1 (The R Foundation for Statistical Computing). Differences in miR-130b expression between tumour and paired normal tissues were compared by the non-parametric Wilcoxon signed ranked test. All other differences between groups were determined by Mann–Whitney *U* test. Spearman's coefficient of correlation (*r*) was used to calculate the correlation between continuous variables. Polyserial correlation coefficient was computed between a continuous and a categorical variable, whereas polychoric was determined when both variables were categorical. The results were considered to be statistically significant at $p < 0.05$.

3. Results

3.1. Consensus from four bioinformatic algorithms identifies 10 candidate miRNAs that bind to RUNX3 3′UTR

The four algorithms (TargetScan, PicTar, miRanda, miRbase Target) used to predict miRNA binding to the 3′UTR of RUNX3 identified 32, 7, 21 and 17 candidate miRNAs, respectively (Supplementary Table 1). Greater specificity in miRNA prediction can be attained by using the consensus of multiple algorithms[23] and hence miRNA predicted to bind to RUNX3 by at least two algorithms was selected for further study. Ten miRNA were selected using this criterion: miR-19a, 19b, 130a, 130b, 301a, 301b, 326, 330-3p, 454 and 495.

3.2. Expression of miR-130b correlates inversely with RUNX3 protein and gene expression in gastric cancer cell lines

To select miRNAs for further analysis, candidate miRNA levels were correlated with RUNX3 protein and mRNA levels in eight gastric cancer cell lines. Of the 10 candidate miRNAs, the expression levels of six were significantly associated with RUNX3 protein levels (Table 1, Fig. 1a). However, only miR-130b was significantly correlated with RUNX3 mRNA

Table 1 – Levels of candidate microRNAs in gastric cancer cell lines and their correlation with RUNX3 mRNA and protein levels.

RNA	Cell lines								Correlation with protein (Polyserial analysis)		Correlation with mRNA (Spearman's rank test)	
	AGS	AZ521	MKN7	MKN28	MKN45	SNU1	SNU5	SNU16	Co-efficient	*p*-Value	Co-efficient	*p*-Value
RUNX3 protein	0	0	0	0	2	0	3	2				
RUNX3 mRNA	0.001	0.555	0.021	0.000	0.779	0.000	1.000	0.507				
miR-19a	1.292	0.847	0.420	0.737	0.629	0.369	1.000	1.366	0.431	0.083	0.265	0.525
miR-19b	1.110	2.297	0.390	0.768	0.801	0.328	1.000	1.329	0.234	0.267	0.402	0.323
miR-130a	13.454	19.835	43.111	0.266	0.094	15.455	1.000	0.135	–0.636	0.006	–0.477	0.232
miR-130b	3.864	1.753	2.713	4.199	1.117	3.227	1.000	1.516	–0.880	<0.001	–0.921	0.001
miR-301a	5.979	7.013	5.169	10.339	6.453	9.318	1.000	3.340	–0.727	0.001	–0.662	0.073
miR-301b	8.634	8.754	5.205	15.780	10.126	14.825	1.000	4.925	–0.651	0.004	–0.593	0.121
miR-326	3.095	2.497	2.329	25.992	7.311	5.205	1.000	6.774	–0.256	0.236	–0.342	0.408
miR-330-3p	30.696	14.723	5.816	14.723	15.032	0.074	1.000	18.896	0.011	0.490	–0.192	0.648
miR-454	1.050	1.424	1.454	1.932	0.889	1.866	1.000	0.753	–0.758	<0.001	–0.647	0.083
miR-495	0.518	0.829	0.183	1.000	0.818	0.586	1.000	0.847	0.573	0.022	0.586	0.127

RUNX3 protein is scored according to band intensity: 0 = negative, 1 = faint, 2 = moderate, 3 = strong.
mRNA and microRNA quantities are relative to SNU5 (set to 1 as a calibrator).

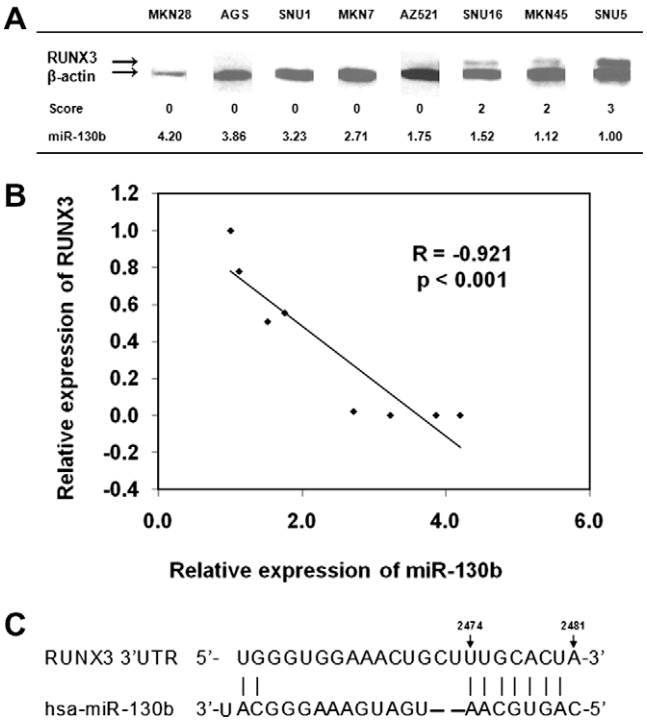

Fig. 1 – (A) Correlation between RUNX3 protein expression and miR-130b levels in gastric cancer cell lines. Scoring of RUNX3 band intensity: 0 = no band, 1 = weak, 2 = moderate, 3 = strong intensity. R = –0.947, $p < 0.001$ by polyserial correlation. (B) Correlation between miR-130b and RUNX3 mRNA levels in gastric cancer cell lines. R = –0.921, $p < 0.001$ by Spearman correlation. (C) Predicted miR-130b-binding site within the 3′UTR of the human RUNX3 gene. The numbers indicate the nucleotide position in reference to the start of the RUNX3 3′UTR.

($p < 0.001$, Table 1, Fig. 1b) and on this basis was selected for further investigation.

3.3. *Overexpression of miR-130b downregulates RUNX3 protein in gastric cancer cell lines*

To examine the effects of miR-130b on RUNX3, miR-130b precursors were transfected into SNU5 cells and the cells were monitored for miR-130b and RUNX3 protein and mRNA levels. RT-qPCR analysis showed that miR-130b levels gradually increased over time and peaked at approximately 36 h after transfection, followed by a sharp decline thereafter (Fig. 2a). Consistent with this pattern, RUNX3 protein levels decreased markedly at 72 h in the cells transfected with miR-130b precursors and then increased at 96 h (Fig. 2b). In contrast, no such changes were observed in the cells transfected with control precursors. Interestingly, no significant change was observed in RUNX3 mRNA levels between the cells transfected with miR-130b or control precursors (results not shown). This suggests that reduction of protein translation rather than mRNA degradation may be the main mechanism by which miR-130b regulates RUNX3. Similar observations were made using the SNU16 cell line (results not shown).

3.4. *Overexpression of miR-130b attenuates apoptosis and increases cell viability following TGF-β treatment*

RUNX3 is involved in mediating TGF-β-induced apoptosis in SNU16 gastric cancer cells.[2] Therefore, to examine the effects of miR-130b on RUNX3 function, precursors and inhibitors were transfected into SNU16 cells treated with TGF-β and then monitored for cell viability, metabolism/proliferation and apoptosis. Using the trypan blue cell assay, higher numbers of viable cells were observed 104–120 h after transfection with miR-130b precursors compared to controls (Fig. 3a). Using the MTS assay, cell proliferation was significantly higher in the cells transfected with precursors compared to controls at 96 h after transfection ($p = 0.03$), but not after 72 h. This result is consistent with the marked decrease in RUNX3 protein expression at 72 h and the probable lag time required to influence cell proliferation (Fig. 3b). Flow cytometry using

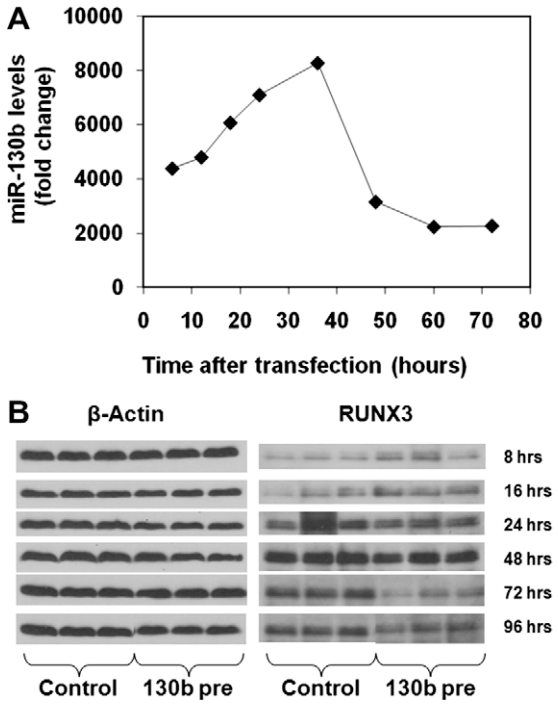

Fig. 2 – (A) Temporal study of miR-130b levels in SNU5 cells transfected with 25 nM of miR-130b miRNA precursor molecules. The results are expressed as fold changes. (B) Western blot analysis of RUNX3 protein expression in SNU5 cells transfected with 25 nM of miR-130b miRNA precursor molecules. Downregulation of RUNX3 was detected 72 h after transfection. Partial restoration of RUNX3 expression was observed at 96 h as the levels of miR-130b began to decrease.

propidium iodide staining and annexin-V binding showed a trend for lower incidence of cell death in TGF-β-treated cells transfected with miR-130b precursors (27.5% ± 0.6) compared to controls (32.2% ± 1.4) ($p = 0.10$; Fig. 3c). In contrast, no differences were observed in cell viability (Fig. 3a) or proliferation (Fig. 3b) in the cells transfected with inhibitors compared to controls.

3.5. *Overexpression of miR-130b downregulates Bim, an immediate downstream pro-apoptotic target of RUNX3, following TGF-β treatment*

During TGF-β-induced apoptosis, one of the major targets for transcription regulation by RUNX3 is the pro-apoptotic protein Bim.[5] Decreased expression of *Bim*, including *BimL* + *BimEL* ($p = 0.10$) and *Bim* splicing variants ($p = 0.01$) compared to controls was observed 72 h after transfection of SNU16 cells with miR-130b precursor molecules and 8 h after the addition of TGF-β. The opposite effects on *Bim* gene expression were observed when the cells were transfected with miR-130b inhibitor molecules, although the differences were not significant (Fig. 3d). However, no changes in Bim protein expression were detected using Western blot when the cells were transfected with either precursor or inhibitor molecules (results not shown).

3.6. *miR-130b expression in gastric cancers correlates inversely with RUNX3 hypermethylation and is expressed at higher levels compared to that in normal tissue*

miR-130b levels were measured in 15 primary gastric tumours and matched with those in normal tissues, together with RUNX3 protein expression and methylation. Nine tumours (60%) showed reduced nuclear RUNX3 expression, 8 (53%) showed cytoplasmic mislocalisation, 6 (40%) showed RUNX3 hypermethylation and 8 (53%) showed overexpression of miR-130b (Table 2). There were no significant associations between any of these factors, with the exception of a strong inverse relationship between miR-130b overexpression and hypermethylation ($p < 0.001$). For the nine cases with reduced RUNX3 nuclear expression, 1 (11%) showed RUNX3 hypermethylation and miR-130b overexpression, 2 (22%) showed neither, 3 (33%) showed hypermethylation only and 3 (33%) showed miR-130b overexpression only. Finally, comparison of tumour and matched normal tissue showed miR-130b to be significantly overexpressed in tumours ($p = 0.017$).

4. Discussion

Accumulating evidence indicates that miRNA repression of tumour suppressor genes may be a common mechanism involved in tumourigenesis, including the regulation of RB1 by miR-106a[24] and PTEN by miR-21.[25] Aberrant expression of a growing number of miRNAs has also been linked to the development of gastric cancer. These include upregulation of miR-21 which targets RECK,[26] an anti-metastasis factor, and upregulation of miR-27a which targets prohibitin,[27] a negative regulator of cell proliferation.

In this study, a bioinformatics approach was used to first identify miRNAs that are predicted to bind to RUNX3. Not all miRNAs identified in this manner are likely to be functional since factors such as steric hindrance may render them inaccessible to the mRNA. Hence, functional validation and assessment in clinical samples are needed. miR-130b was selected as the best candidate for studying miRNA regulation of RUNX3 based on the consensus from four alignment algorithms (Supplementary Table 1) and following correlation with RUNX3 protein and RNA levels (Fig. 1, Table 1).

The human miRNA-130b stem-loop sequence (miRBase accession number MI0000748) codes for a mature sequence of 22 bases in length (5′-cagugcaaugaugaaagggcau-3′; miRBase accession number MIMAT0000691). Its seed region binds to nucleotides 2474–2481 of the 3′UTR of RUNX3 mRNA (Fig. 1C), suggesting the capacity for miR-130b to bind directly to RUNX3 mRNA. Experiments involving the transfection of miR-130b precursors showed that miR-130b can downregulate RUNX3 protein expression in gastric cancer cell lines (Fig. 2) and influence well-established RUNX3-mediated effects of TGF-β on cell viability, proliferation and transcription (Fig. 3). These results indicate that miR-130b can bind to RUNX3, downregulate its expression and affect its downstream activities. Together, they provide evidence that miR-130b may be an active epigenetic mechanism in the regulation of RUNX3 expression.

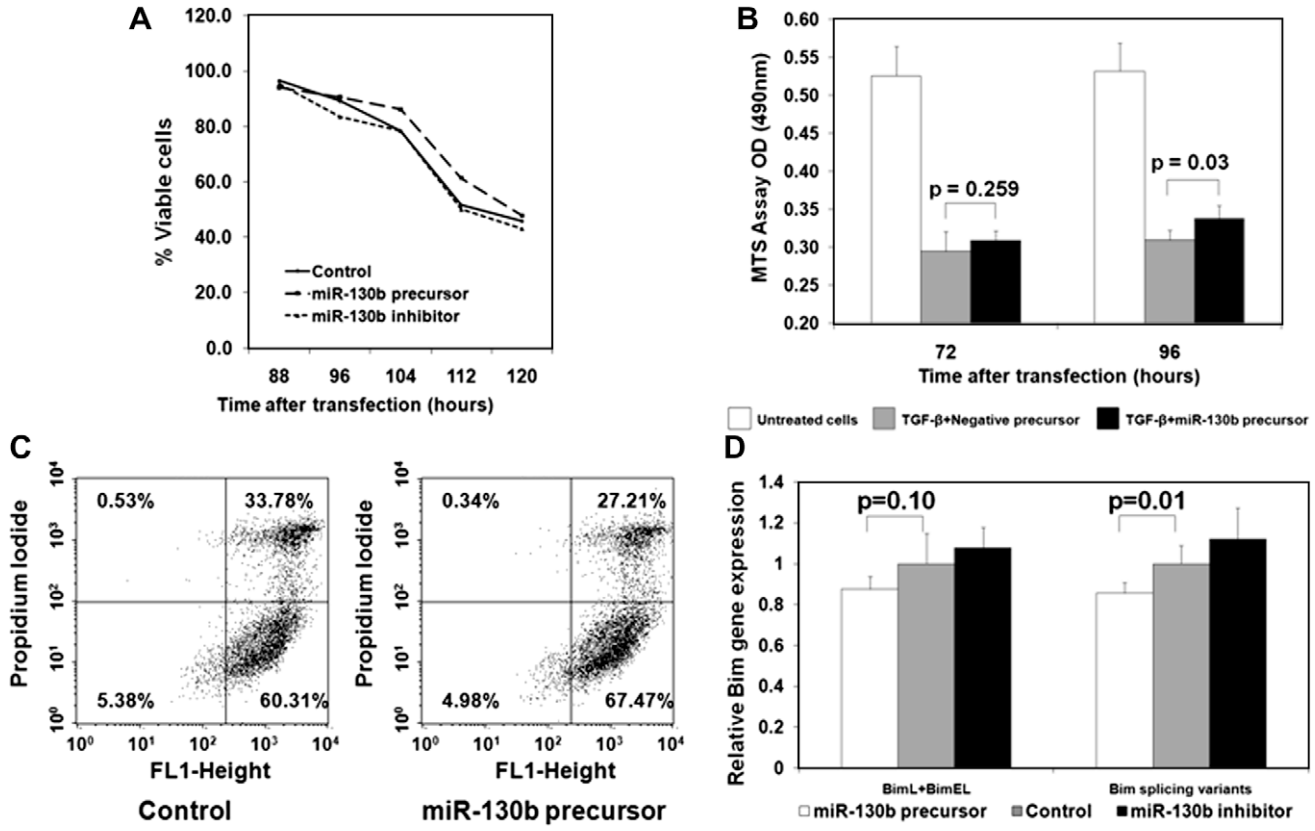

Fig. 3 – (A) Cell viability analysis by trypan blue cell count. The results are the mean of 3 repeats and are expressed as a percentage of viable cells amongst the total cells counted. (B) MTS cell proliferation assay. A significant increase in cell proliferation was observed 96 h after transfection with 25 nM of miR-130b precursor when compared to negative precursor control, 24 h after downregulation of the RUNX3 protein. The results are expressed as mean ± SD, *p*-values are derived from Mann–Whitney test, *n* = 6 for each group. (C) FACS analysis of apoptosis by propidium iodide staining of SNU16 cells treated with TGF-β. Increased cell death was observed in controls (*n* = 3) when compared with cells treated with miR-130b precursor (*n* = 3). (D) Relative gene expression of *Bim* (*BimL* + *BimEL* and *Bim* splicing variants) as determined by RT-qPCR in SNU16 cells undergoing TGF-β mediated apoptosis. The cells were transfected with either 25 nM of miR-130b precursor or 50 nM of miR-130b inhibitor. The results are expressed as mean ± SD, *p*-values are derived from Mann–Whitney test, *n* = 6 in each group.

Table 2 – RUNX3 nuclear and cytoplasmic protein expression, DNA methylation and miR-130b levels in gastric tumour and normal tissue.

Case	Tumour				Normal tissue	
	Nuclear expression	Cytoplasmic expression	DNA methylation	miR-130b	DNA methylation	miR-130b
3	3 (+)	Absent (–)	30.7 (+)	1.0 (–)	0.2 (–)	2.0 (–)
15	3 (+)	Present (+)	25.2 (+)	4.4 (–)	0.6 (–)	1.9 (–)
9	3 (+)	Present (+)	1.3 (–)	13.4 (+)	0.7 (–)	7.4 (–)
7	3 (+)	Absent (–)	0.1 (–)	27.9 (+)	0.0 (–)	16.6 (+)
11	3 (+)	Absent (–)	0.0 (–)	9.2 (+)	0.0 (–)	4.2 (–)
6	3 (+)	Absent (–)	0.0 (–)	32.7 (+)	0.1 (–)	7.2 (–)
12	2 (–)	Present (+)	6.5 (+)	8.2 (+)	0.0 (–)	1.1 (–)
13	2 (–)	Present (+)	4.5 (+)	7.1 (–)	0.1 (–)	7.6 (–)
2	0 (–)	Present (+)	24.6 (+)	4.2 (–)	4.2 (+)	15.4 (+)
4	0 (–)	Absent (–)	121.1 (+)	4.8 (–)	4.0 (+)	2.1 (–)
14	2 (–)	Absent (–)	0.6 (–)	18.6 (+)	5.8 (+)	13.0 (+)
1	2 (–)	Present (+)	0.4 (–)	8.7 (+)	0.2 (–)	2.2 (–)
8	1 (–)	Absent (–)	0.8 (–)	30.6 (+)	10.1 (+)	13.9 (+)
5	1 (–)	Present (+)	0.7 (–)	7.5 (–)	0.1 (–)	3.9 (–)
10	0 (–)	Present (–)	0.1 (–)	5.9 (–)	1.3 (–)	6.4 (–)

Positive (+) and negative (–) classifications according to the thresholds described in Section 2.

Overexpression of miR-130b in primary gastric tumours was observed to occur at the same frequency (53%) as RUNX3 cytoplasmic mislocalisation (53%) and at a higher frequency than RUNX3 hypermethylation (40%), suggesting that it could play a significant role in RUNX3 inactivation. Most notably, miR-130b overexpression was inversely associated with RUNX3 hypermethylation, suggesting that it may be an alternative mechanism for silencing RUNX3 (Table 2). Hypermethylation is currently the most commonly reported mechanism of RUNX3 suppression in cancer;[28] however, cases of RUNX3 downregulation without hypermethylation are frequently observed. The overexpression of miR-130b may provide a plausible explanation for these cases. The present results also imply that RUNX3 could be inactivated in a larger proportion of cancers than is currently considered.

In contrast to other loss-of-function studies that have used antisense nucleotides, no change was detected in RUNX3 expression or biological function in the cells treated with miR-130b inhibitor molecules (Fig. 3b). This was despite a reduction of over 80% in the miR-130b level compared to the control (result not shown). miR-130b shares the same seed sequence with miR-130a, 301a and 301b, which together with miR-454 belong to the same miRNA family in the human genome and may have common binding targets. In fact, miR-301b is within 10 kb of miR-130b on chromosome 22, suggesting that they may be expressed in tandem and share similar biological roles in the cell. A recent study of miRNA cluster miR-106b~93~25 demonstrated that the members of this family have related biological functions in the suppression of Cdk inhibitors.[29] The strong inverse correlations of miR-301a, -301b and -454 with RUNX3 expression (Table 1) may explain why the inhibition of miR-130b alone did not lead to increased RUNX3 expression or alter its downstream functions. The use of multiple miRNA inhibitor molecules that act on the members of the same miRNA family or miRNA clusters warrants further investigation.

Recently, miR-532-5p was reported to regulate RUNX3 expression in cutaneous melanoma.[30] miR-532-5p expression was upregulated in melanoma cell lines and metastatic melanoma tumours. Transfection of anti-miR-532-5p molecules in melanoma cell lines upregulated both RUNX3 mRNA and protein expression, although possible effects on downstream RUNX3 activities or of transfection with precursor molecules were not studied. miR-532-5p was not identified as a consensus miRNA in interrogation of four miRNA alignment algorithms, and hence not a top candidate for the current study. Nevertheless, the work by Kitago and colleagues and the results of this study support the notion that miRNA is an epigenetic mechanism for the regulation of RUNX3, although possibly with different miRNAs involved in different cancer types.

In conclusion, the results of this study indicate that, in addition to hypermethylation, histone modification, cytoplasmic mislocalisation and hemizygous deletion, RUNX3 can also be inactivated in cancer cells by miRNA expression, possibly as an alternative mechanism to hypermethylation. Further studies should reveal whether other miRNAs play a role in RUNX3 suppression in gastric cancer and whether this is a common mechanism in human tumourigenesis.

Conflict of interest statement

None declared.

Acknowledgements

This study was supported by grants from the National Medical Research Council of Singapore (NMRC/TCR/001/2007), the Singapore Cancer Syndicate (SCS#BU51), and the Singapore National Research Foundation and the Ministry of Education under the Research Center of Excellence Programme.

Appendix A. Supplementary material

Supplementary data associated with this article can be found, in the online version, at doi:10.1016/j.ejca.2010.01.036.

REFERENCES

1. Ito K, Lim AC, Salto-Tellez M, et al. RUNX3 attenuates beta-catenin/T cell factors in intestinal tumorigenesis. *Cancer Cell* 2008;**14**(3):226–37.
2. Li QL, Ito K, Sakakura C, et al. Causal relationship between the loss of RUNX3 expression and gastric cancer. *Cell* 2002;**109**(1):113–24.
3. Vogiatzi P, De Falco G, Claudio PP, Giordano A. How does the human RUNX3 gene induce apoptosis in gastric cancer? Latest data, reflections and reactions. *Cancer Biol Ther* 2006;**5**(4):371–4.
4. Chi XZ, Yang JO, Lee KY, et al. RUNX3 suppresses gastric epithelial cell growth by inducing p21(WAF1/Cip1) expression in cooperation with transforming growth factor {beta}-activated SMAD. *Mol Cell Biol* 2005;**25**(18): 8097–107.
5. Yano T, Ito K, Fukamachi H, et al. The RUNX3 tumor suppressor upregulates Bim in gastric epithelial cells undergoing transforming growth factor beta-induced apoptosis. *Mol Cell Biol* 2006;**26**(12):4474–88.
6. Soong R, Shah N, Peh BK, et al. The expression of RUNX3 in colorectal cancer is associated with disease stage and patient outcome. *Br J Cancer* 2009;**100**(5):676–9.
7. Subramaniam MM, Chan JY, Soong R, et al. RUNX3 inactivation by frequent promoter hypermethylation and protein mislocalization constitute an early event in breast cancer progression. *Breast Cancer Res Treat* 2009;**113**(1):113–21.
8. Yoshizaki T, Enomoto T, Fujita M, et al. Frequent inactivation of RUNX3 in endometrial carcinoma. *Gynecol Oncol* 2008;**110**(3):439–44.
9. Gao F, Huang C, Lin M, et al. Frequent inactivation of RUNX3 by promoter hypermethylation and protein mislocalization in oral squamous cell carcinomas. *J Cancer Res Clin Oncol* 2009;**135**(5):739–47.
10. Sakakura C, Miyagawa K, Fukuda KI, et al. Frequent silencing of RUNX3 in esophageal squamous cell carcinomas is associated with radioresistance and poor prognosis. *Oncogene* 2007;**26**(40):5927–38.
11. Sugiura H, Ishiguro H, Kuwabara Y, et al. Decreased expression of RUNX3 is correlated with tumor progression

and poor prognosis in patients with esophageal squamous cell carcinoma. *Oncol Rep* 2008;**19**(3):713–9.
12. Ito K, Liu Q, Salto-Tellez M, et al. RUNX3, a novel tumor suppressor, is frequently inactivated in gastric cancer by protein mislocalization. *Cancer Res* 2005;**65**(17):7743–50.
13. Fujii S, Ito K, Ito Y, Ochiai A. Enhancer of zeste homologue 2 (EZH2) down-regulates RUNX3 by increasing histone H3 methylation. *J Biol Chem* 2008;**283**(25):17324–32.
14. Xiao WH, Liu WW. Hemizygous deletion and hypermethylation of RUNX3 gene in hepatocellular carcinoma. *World J Gastroenterol* 2004;**10**(3):376–80.
15. Lagos-Quintana M, Rauhut R, Lendeckel W, Tuschl T. Identification of novel genes coding for small expressed RNAs. *Science* 2001;**294**(5543):853–8.
16. Brodersen P, Voinnet O. Revisiting the principles of microRNA target recognition and mode of action. *Nat Rev Mol Cell Biol* 2009;**10**(2):141–8.
17. Croce CM. Causes and consequences of microRNA dysregulation in cancer. *Nat Rev Genet* 2009;**10**(10):704–14.
18. Johnson SM, Grosshans H, Shingara J, et al. RAS is regulated by the let-7 microRNA family. *Cell* 2005;**120**(5):635–47.
19. Meng F, Henson R, Wehbe-Janek H, et al. MicroRNA-21 regulates expression of the PTEN tumor suppressor gene in human hepatocellular cancer. *Gastroenterology* 2007;**133**(2):647–58.
20. Griffiths-Jones S, Grocock RJ, van Dongen S, Bateman A, Enright AJ. miRBase: microRNA sequences, targets and gene nomenclature. *Nucleic Acids Res* 2006;**34** (database issue):D140–4.
21. Soong R, Iacopetta BJ. A rapid and nonisotopic method for the screening and sequencing of p53 gene mutations in formalin-fixed, paraffin-embedded tumors. *Mod Pathol* 1997;**10**(3):252–8.
22. Weisenberger DJ, Siegmund KD, Campan M, et al. CpG island methylator phenotype underlies sporadic microsatellite instability and is tightly associated with BRAF mutation in colorectal cancer. *Nat Genet* 2006;**38**(7): 787–93.
23. Kuhn DE, Martin MM, Feldman DS, et al. Experimental validation of miRNA targets. *Methods* 2008;**44**(1):47–54.
24. Volinia S, Calin GA, Liu CG, et al. A microRNA expression signature of human solid tumors defines cancer gene targets. *Proc Natl Acad Sci USA* 2006;**103**(7):2257–61.
25. Talotta F, Cimmino A, Matarazzo MR, et al. An autoregulatory loop mediated by miR-21 and PDCD4 controls the AP-1 activity in RAS transformation. *Oncogene* 2009;**28**(1):73–84.
26. Zhang Z, Li Z, Gao C, et al. MiR-21 plays a pivotal role in gastric cancer pathogenesis and progression. *Lab Invest* 2008;**88**(12):1358–66.
27. Liu T, Tang H, Lang Y, Liu M, Li X. MicroRNA-27a functions as an oncogene in gastric adenocarcinoma by targeting prohibitin. *Cancer Lett* 2009;**273**(2):233–42.
28. Kim TY, Lee HJ, Hwang KS, et al. Methylation of RUNX3 in various types of human cancers and premalignant stages of gastric carcinoma. *Lab Invest* 2004;**84**(4): 479–84.
29. Kim YK, Yu J, Han TS, et al. Functional links between clustered microRNAs: suppression of cell-cycle inhibitors by microRNA clusters in gastric cancer. *Nucleic Acids Res* 2009;**37**(5):1672–81.
30. Kitago M, Martinez SR, Nakamura T, Sim MS, Hoon DS. Regulation of RUNX3 tumor suppressor gene expression in cutaneous melanoma. *Clin Cancer Res* 2009;**15**(9): 2988–94.